Published by :
http://www.ijert.org

International Journal of Engineering Research & Technology (IJERT)
ISSN: 2278-0181
Vol. 10 Issue 11, November-2021

Enhanced Invasive Ductal Carcinoma Prediction Using Densely Connected Convolutional Networks

Fred Lubega
Department of Information Science and Technology
Zhejiang Sci-Tech University
Hangzhou, China

Shen Wei
Department of Information Science and Technology
Zhejiang Sci-Tech University
Hangzhou, China

Al-Selwi Metwalli
Quanzhou Institute of Equipment Manufacturing
Chinese Academy of Sciences
Fujian, China

***Abstract*—Breast cancer is a heterogeneous disease that occurs when malignant cells form in the breast. It is the most common type of cancer in women but, it can also affect men. Due to its invasiveness and frequency of occurrence, breast cancer can be hard to diagnose. Although several approaches utilizing digital pathology and deep learning methods have successfully addressed the issue, these methods fail to capture some intrinsic and extrinsic cellular structural features required for precise automatic detection of Invasive Ductal Carcinoma (IDC) of the breast. Our proposed DenseBreast methodology involves the diagnosis of invasive ductal carcinoma with a densely connected convolutional network (DenseNet) to classify the IDC-affected histopathology images from the normal images. The benchmark dataset thus used to perform this task is the Breast Histopathology Images. The RGB microscopic images are first enhanced through our hybrid pre-processing technique based on color normalization, denoising, adaptive gamma correction (AGC), and contrast limited adaptive histogram equalization (CLAHE) with a 9% image quality improvement compared to the commonly used color normalization by Macenko. These images are then fed to the network which achieves an accuracy of 90%, a balanced accuracy of 87.2%, an improved f-score of 88.0%, and sensitivity/specificity of 80/95 % on a reduced dataset. Classification aptitude of the model is tested using standard performance metrics.**

Keywords*—DenseNets, Digital pathology, Grad CAM, Adaptive Gamma Correction, Median filtering, Color Normalization, Breast cancer histopathology.

I. INTRODUCTION

In women, 2.1 million of them get affected each year by breast cancer which is the most prevalent form of cancer and the cause of cancer deaths globally according to the World Health Organisation (WHO) [1]. Invasive ductal carcinoma (IDC), also known as infiltrating carcinoma, is the most common phenotypic subtype, accounting for nearly 80% of all breast cancer cases [2], [3]. This form of invasive breast cancer originates in the lining of the milk ducts and soon invades the tissue of the breast outside the duct as shown in Figure 1. A medical test, usually performed by surgeons, is required to

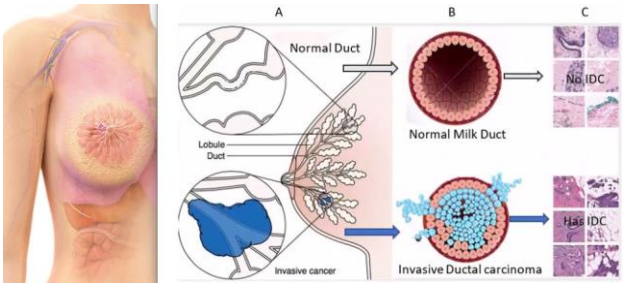

Fig. 1 A. An illustration of a normal duct and affected duct with invasive cancer. B. Cross-sectional area of both normal duct and affected duct with invasive cancer. C. shows the digitized images of the normal and affected ducts (biopsies).

diagnose the disease, followed by a microscopic examination of breast tissue. In the first stage of this process, surgeons cut section biopsy samples and then stain them with hematoxylin and eosin staining. The hematoxylin binds to deoxyribonucleic acid (DNA) and highlights nuclei, whereas eosin binds to proteins and highlights other structures [4]. In the second stage of this analysis, they examine tissue biopsies by visualizing highlighted regions in digitized images using microscopes to distinguish between tissue regions corresponding to an invasive tumor and non-invasive or healthy tissues. The examination of tissue biopsies allows the identification of their early clues. However, professional surgeons must spend considerable time and effort to accomplish this task. This is not only time-consuming and costly, but it also heavily relies on the surgeons' prior knowledge and the consistency of pathology reports dealing with a wide variety of hematoxylin and eosin-stained sections, which are attributed to differences among people, different lab protocols, and different staining procedures. [5]–[7]. High-resolution whole slide images (WSI) can be generated with a microscope slide digitized using digital scanners. Utilizing advanced image detection and pattern recognition algorithms, automatic image processing can then be employed to detect IDC in whole slide images (WSI) [8], [9]. One

International Journal of Engineering Research & Technology (IJERT)
ISSN: 2278-0181
Vol. 10 Issue 11, November-2021

challenge with these algorithms is that their performance is highly dependent on the staining process and the quality of stained slides used. [10], [11]. To meet this challenge, we first enhance the images through our hybrid pre-processing technique based on color normalization, denoising, adaptive gamma correction, and contrast limited adaptive histogram equalization (CLAHE) which feeds into the automated breast cancer classification detector to classify breast tissues precisely into normal and abnormal cells ensuring accurate diagnosis and the most appropriate course of therapy as shown in Fig.2. The dataset used for this purpose consisted of breast cancer histopathology images with very low-resolution and contained impulse noise which made its analysis challenging. The image slides are whole slide images patched and stained with hematoxylin and eosin staining. However, this staining is not uniform in all images as some images are corrupted. The proposed model is based on the concepts of densely connected convolutional neural networks, which alleviate the vanishing-gradient problem, strengthen feature propagation, encourage feature reuse, and significantly reduce the number of parameters. To achieve the best performance results and to overcome the challenge of staining, poor resolution and impulse noise in histopathology images we resized the images, applied a color normalization algorithm, denoising utilizing median blurring algorithm, adaptive gamma correction, followed by contrast limited adaptive histogram equalization (CLAHE) which accurately removed the artifacts, maintaining the contrast ratio in the images. The validity of the proposed model was finally tested using GRADCAM visualization for the convolution layers and the fully connected (FC) layers. The rest of this paper is organized as follows: Section. II presents the literature review; Section. III explains in details the proposed methodology; Section. IV discusses the results obtained by the model. Finally, Section. V concludes with the main findings and discusses its future scope.

II. LITERATURE REVIEW

In recent years, supervised learning based classification on Invasive Ductal Carcinoma (IDC) in breast cancer histopathology images has received increasing research attention in the community of machine learning [12]. The methods using deep learning and especially convolutional neural networks (CNN) [13], [14], have been the most successful so far in processing the task of carcinoma detection in histopathology images. However, convolutional neural networks have their own uniqueness, such as revealing the conserved spatial correlation within tumor histological images [15]. Y. Lecun et al. [16] for the first time formulated a character detection problem explicitly. They proposed the concept of gradient based learning and then presented it to different neural networks, forming the core foundation of convolutional neural networks used in histopathology image processing today.

Nuclei detection and segmentation are defined in [17] which aids in the understanding of the methods to deal with nuclei complex structures in histopathology images. Equally important, Huang et al. [18]. proposed a Densely Connected Convolutional Network that improved information flow between layers and boosted their performance on deeper networks without the issue of vanishing gradients. This learning methodology is also employed in our proposed method. In addition, K. Lan et al [19]. discuss several deep learning exemplars and data mining

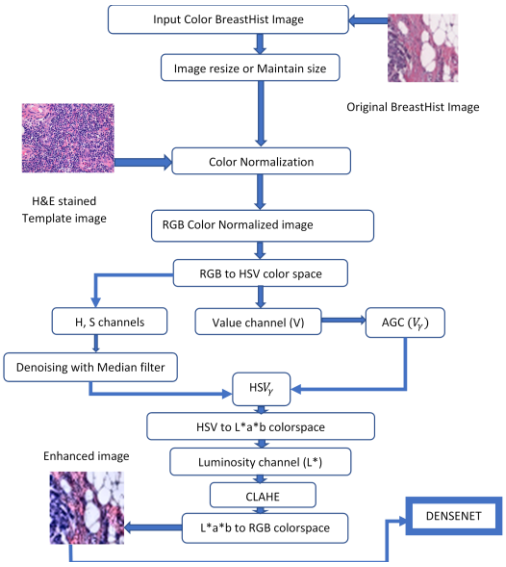

Fig. 2 Proposed DenseBreast methodology for classifying breast tumours

methods, as well as the importance of data preprocessing and transformation in bioinformatics. Network that improved information flow between layers and boosted their performance on deeper networks without the issue of vanishing gradients. This learning methodology is also employed in our proposed method. In addition, K. Lan et al [19]. discuss several deep learning exemplars and data mining methods, as well as the importance of data preprocessing and transformation in bioinformatics. As a result, the classification of histopathology images has also benefited from image processing and analysis, along with machine learning approaches that enable image search, which depicts a fundamental shift in computational pathology [20]. S. Doyle et al. [21] proposed an image processing approach for identifying low-grade and high-grade breast cancer from histopathology images. In the same way, S. Naik et al. [22] defined a system for classifying prostate and breast cancer histopathology images utilizing gland and nuclear segmentation. To make use of the pixel data, a level-set algorithm, a template matching algorithm, and a Bayesian classifier are employed to utilize the pixel information at different scales. For histopathology image recognition in class-imbalanced data, M. S. Reza and J. Ma [23] employ a combination of sampling techniques and convolutional neural networks for histopathology image classification in class-imbalanced data. E. Bejnordi et al. [24] also presented an algorithm for detecting DCIS in histopathological slides of breast tissue stained with hematoxylin and eosin (H&E). To differentiate DCIS from a large set of set conditions, this method employs a multi-scale super pixel classification on whole slide images (WSLs). M. Balazi et al. [23] suggested a method for identifying IDC-expressing regions in microscopic tissue images or whole digital slides and Vo et al [24] in their publication suggest a novel boosting approach in which the method is effectively enriched by gradually merging weak classifiers into a stronger classifier. Their method divides hematoxylin and eosin-stained breast biopsy images into two categories: carcinomas and non-carcinomas. Similarly, B. E. Bejnordi et al. [25] also suggest a new approach for identifying invasive ductal carcinomas in whole-slide histopathology images. The approach suggests piling two CNNs on top of one another, with the first CNN's feature maps being fed into the

International Journal of Engineering Research & Technology (IJERT)
ISSN: 2278-0181
Vol. 10 Issue 11, November-2021

second CNN. This method achieves a three-class accuracy of 81.3% for the classification of WSIs into normal or benign, DCIS, and IDC.

Furthermore, in digital histopathology, data preprocessing is a method dealing with the data before the main operation, tasks of classification and disease diagnosis are accomplished through quantitative examination of image data. However, the color variance caused by uneven biopsy staining and nonstandard imaging conditions in image samples makes it difficult to obtain precise results. According to [26] a preprocessing step is introduced as an important step in the overall process to overcome color variation problems in histopathology images. Contrast enhancement and brightness preservation are critical image quality control steps for creating informative and visually appealing images [27], [28]. In most cases, a histogram equalization-based image enhancement tool is utilized, however, it does not provide better contrast enhancement or brightness preservation. When it comes to medical images, this could lead to a loss of diagnostic information. An attempt was made to integrate histogram equalization with gamma correction to study the improvement in contrast while preserving the essential details of the image. [29]. Finally, recent advancements in the Densely Connected Convolutional Networks (DenseNet) architecture [18] have facilitated the use of neural network applications that focus on improving image quality through reconstruction in terms of resolution or dynamic range. The authors demonstrate the ability of the architecture to classify images. The concept of dense connections has influenced deep learning in a variety of ways. As a result, the DenseNet architecture has been widely adopted and has proven to be effective for a variety of tasks [30]. However, in the field of histopathology image analysis, they fail to capture and incorporate the most intrinsic and extrinsic structural or molecular behavior of the images, resulting in a higher rate of false-positive and false-negative results.

III. PROPOSED METHODOLOGY

Deep learning algorithms process data through multiple layers of neural network algorithms, each of which transfers a simpler representation of the data to the next layer, learning more about the input data (image) as it passes through each layer. The dataset in question consists of histopathological images of normal and affected breast cancer cells. The proposed model is based on the use of 2D Convolutional layers to build the densely connected convolutional neural networks. Along with the model, a detailed preprocessing of the images is proposed, which involves a hybrid feature preservation strategy focused on luminosity and edge contrast enhancement. Our approach also utilizes paradigms to avoid the dangers of increasing loss (caused by the vanishing gradient problem) as the model's depth increases. The dataset preparation, data preprocessing procedure, and model development are all covered extensively in the sections below.

A. *Dataset Preparation*

The Kaggle Breast Cancer Histopathology Images[31]. supported the dataset for this study. 162 whole mount slide images of Breast Cancer (BCa) specimens were scanned at 40x in the initial dataset. With a zoom factor of 2.5x (4m/pixel), 277,524 patches of size 50 x 50 were extracted. 198,738 images were found to be IDC negative, while 78,786 were found to be IDC positive. The proposed methodology was tested on a subset of 250757 images, with 78786 IDC positive images and 171971 IDC negative images. Since some images were corrupt for execution, their amount reduced after our data preprocessing method.

B. *Data Preprocessing*

The images had a lower resolution of (50 x 50), thus they were resized to (100 x 100) dimensions to fit the model. This resizing was accompanied by image color normalization and denoising using the median blur algorithm on the two HSV colorspace channels of hue and saturation. In HSV colorspace, adaptive gamma correction was applied to the image's value channel, followed by enhancement in L*a*b*colorspace using the CLAHE (contrast limited adaptive histogram equalization). The final RGB transformed image obtained was fed to the model for classification as shown in fig.2.

1) *Color Normalization*

We normalize the amount of H&E stained on the tissue for accurate and reproducible classification of the key tissue components in the image by bringing the microscopy images into a common space. Stain normalization is a color transfer technique between a source (reference) and a test image that aids in resolving an important concern of stain color variance caused by irregularities in the preparation of histology slides that make it difficult to perform quantitative analysis on their results. Color-texture detail is well captured using appropriate features and data with enough color variation. Our approach is based on [32] works according to the algorithm in table.1:

TABLE I. SVD-GEODESIC METHOD FOR OBTAINING STAIN VECTORS

Algorithm 1: SVD-geodesic method for obtaining stain vectors.

1. Input the source and target image and convert the RGB image into lαβ color space.
2. The tolerance for the pseudo-minimum α^{th} and pseudo-maximum $(100-\alpha)^{th}$ percentiles is initialized. It produces better results when $\alpha = 1$, Optical Density (OD) threshold value for transparent pixels $\beta = 0.15$, and the transmitted light intensity $I = 240$ are used.
3. The histopathology image color is converted into the optical density value as shown in equation (A.1)
   Each component is normalized in the range of [0 1], where, 'I' stands for the source image.
   $$OD = -log_{10}(I) \qquad \text{(A.1)}$$
4. A condition is applied on the OD threshold value if the OD threshold value $\beta < 0.15$. and transparent pixels eliminated. For this reason, the optical density values (OD) are divided into two matrices as shown in equation (A.2) and (A.3) respectively.
   $$OD = V * S \qquad \text{(A.2)}$$
   $$S = V' * OD \qquad \text{(A.3)}$$
   Where, OD refers to the optical density values, S is the saturation value of each stain and V is the stain vector matrix.
5. The singular value of the SVD decomposition on the optical density (OD) value is calculated and the optical density values projected onto the plane.
6. The histogram of the angles is obtained after angle calculation in every point with respect to the first singular value decomposition direction and mapping of the direction in the plane.
7. The concentration of the individual stains by using Hematoxylin and Eosin matrix with respect to the OD values are determined and the stain concentration normalized.
8. Finally, the normalized image is obtained from the reference mixing matrix with the normalized stain concentration and executing the HE matrix.

International Journal of Engineering Research & Technology (IJERT)
ISSN: 2278-0181
Vol. 10 Issue 11, November-2021

2) Denoising of Images

Due to the poor Signal to Noise ratio, digital pathology analysis of histopathology images is a difficult process, necessitating the use of filters to minimize noise. This phase, however, typically degrades the quality of the edges of the affected regions in microscopic cells, particularly in IDC positive labeled images, rendering them more diffuse. Furthermore, lens and acquisition device distortions affect these images. As a result, the median blur algorithm, which is an efficient tool for distinguishing out-of-range discrete noise from valid image features such as edges and lines on microscopic images, can be used to enhance the representation of the edge by minimizing distortions. [33]. Using this process, the impulse noise (Pepper and salt noise) is minimized by replacing a pixel with the median rather than the average of all pixels in a neighborhood 'w' as shown below:

$$y[m,n] = median\{x[i,j], (i,j) \in w \qquad (1)$$

The median filter is a pixel-by-pixel image analysis tool, as seen in (1). Where w is the user-defined neighborhood based on the image's position. With a window size of 3x3, the two H and S channels in the HSV colorspace are blurred.

3) Adaptive gamma correction

Owing to the inadequate lighting, the luminance component of the image needed to be improved accordingly. We did so by experimenting with adaptive gamma correction and Blind Inverse Gamma Correction with Maximized Differential Entropy [34] on the value channel (V) of the breast cancer histopathology image in HSV color space, while maintaining the hue (H) and saturation (S) channels intact to prevent color distortion. Based on adaptive gamma correction [35], the gamma correction function is theoretically defined as:

$$V_\gamma = cV^\gamma \qquad (2)$$

Where V_γ denotes the gamma-corrected value channel (V), while c and γ denote the adaptive parameters for shaping the transformation curve using image data. For low contrast images, γ is calculated using (3):

$$\gamma = -log_2(\sigma) \qquad (3)$$

The value of c is given by the equation bellow:

$$c = \frac{l}{1 + H(0.5 - \mu) \times (k - 1)} \qquad (4)$$

Where k is defined as:

$$k = V^\gamma + (1 - V^\gamma) \times \mu^\gamma \qquad (5)$$

and the Heaviside function is represented as shown in (6):

$$H(n) = \begin{cases} 0, & n \le 0 \\ 1, & n > 0 \end{cases} \qquad (6)$$

For moderate contrast images, γ is calculated using (7):

$$\gamma = exp[(1 - (\mu + \sigma)) / 2] \qquad (7)$$

In case of bright images ($\mu > 0.5$), c becomes 1 as $H(x) = 0$, whereas in case of dark images $\mu < 0.5$, c depends k thereby spreading the lower intensity levels into higher intensity levels with steeper transformation curves for images with lower σ.

4) Enhancement of the images

The images were enhanced with the contrast limited adaptive histogram equalization (CLAHE) algorithm to make the area of interest more visible in order to improve the model's efficiency. Only the Luminosity Component L in L*a*b*colorspace was enhanced. Denoising was performed prior to enhancement to eliminate the probability of noise enhancement. An image in the CLAHE algorithm is represented as $f(x,y)$,with histogram as $h(i)$ and its cumulative distribution defined in (8) as follows:

$$H(i) = \int_0^1 h(p)dp \qquad (8)$$

Image enhancement is done using the function defined in (9):

$$g(x,y) = H\big(f(x,y)\big) \qquad (9)$$

Where, g(x, y) is the enhanced image which can be obtained for each Luminosity channel of the image in L*a*b*colorspace.

C. Model Development

The proposed DenseBreast methodology is based on the notion of densely connected convolutional networks with 2D convolutional layers. A three-dimensional RGB breast cancer histopathology image is used as input for the 2D convolutional layers in our model. They inspect a small window of pixels at a time by passing a filter, also known as a convolution kernel, over the image. The dot product of the pixel values in the current filter window with the weights specified in the filter is determined by the convolution operation. This makes 2D-convolutional layers very effective at dealing with image data. In contrast to a network of few layers, the failure saturates at a much higher value as the model depth increases. This effect of decreasing accuracy and saturating loss is termed as vanishing Gradient. As seen in fig.3, our model integrates several methods and skip connections to resolve this problem.

International Journal of Engineering Research & Technology (IJERT)
ISSN: 2278-0181
Vol. 10 Issue 11, November-2021

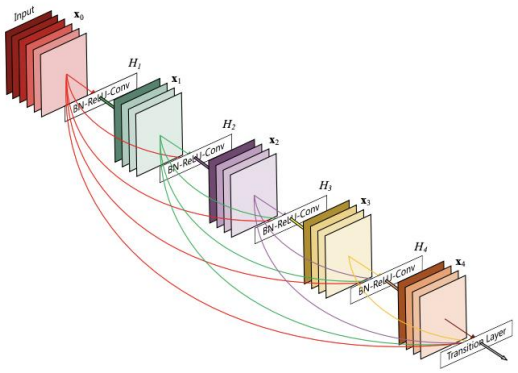

Fig. 3: A dense block of 5-layers with a growth rate of $k = 4$. (Image source Huang et al. [18])

1) DenseBreast Structure: As shown in Fig. 4, the DenseBreast model consists of two major components namely the DenseNet for feature extraction with initial layers, dense block layers, transition layers, and the Extreme gradient boosting for classification trained from scratch as detailed below:

a) Initial Layers: These consist of a convolution layer and a pooling layer to extract the maximum amount of information from the images before they are fed to dense block layers. The feature maps are down-sampled to minimize the number of parameters.

b) Dense Block Layers: The DenseNet structure transfers information between layers using dense connectivity. The Batch normalization, activation function, and a convolution layer make up the dense block. Each layer's output is used as the input for subsequent layers. Thus, the l^{th} layer receives the feature maps from all preceding layers. Consider $x_0, x_1, \ldots, x_{l-1}$ as inputs:

$$x_1 = H_l([x_0, x_1, \ldots, x_{l-1}]), \qquad (10)$$

Where x_l denotes the output of the l^{th} layer, $[x_0, x_1, .., x_{l-1}]$ denotes the combination of the feature maps produced by the preceding l layers 0,1, ……, $l-1$, and $H_l([])$ is a composition function of the operations for batch normalization (BN), exponential linear unit (ELU), and 3x3 Convolution (conv) [43].

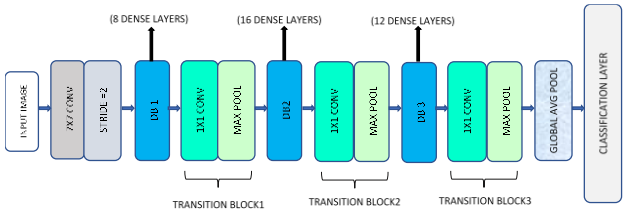

Fig. 4 DenseBreast model consisting of input layer, convolution, pooling, three dense blocks, three transition layers, global average pooling, and a classifier (Fully Connected Layer)

The $H_l()$ function produces k feature maps, where k is a hyper-parameter that refers to the network growth rate, so the l^{th} layer has $k_0 + k_{l-1}$ input feature maps and $\frac{l(l+1)}{2}$ connections instead of l connections as in the other traditional models. The 3x3 convolution layers are used to extract image features, and 1x1 convolutions are used as bottleneck layers. Batch normalization and activation function are used before the convolution. Following [36], we use an ELU activation function, defined as:

$$ELU = \begin{cases} x & if\ x > 0, \\ e^x - 1 & if\ x \le 0, \end{cases} \qquad (11)$$

to speed up learning, tackle the vanishing gradient problem, and improve classification accuracy. The output of each dense block is a concatenation of feature maps totaling $k.H_l$. However, a simple model may not fit the data well and thus suffer from under fitting, while a very deep model may have a high computational cost and thus need a larger dataset to achieve generalizable efficiency [37]. Since our dataset is too small to train a complex model, we built three dense blocks with 8,16, and 12 layers to address these issues as shown in Fig.4.

c) Transition Layers: Convolutional neural networks need down-sampling layers to function properly. We divide the network architecture into four dense blocks to reduce the feature-map dimension. Transition layers are the layers that sit between dense blocks and include batch normalization, ELU, 1x 1 convolution layer, and 2 x 2 max-pooling layer. To minimize dimension features and extract essential features such as edges, we use max-pooling instead of average pooling for down-sampling. It's worth noting that average pooling extracts seem to flow smoothly [38], [39]. To minimize the number of feature maps, prevent over-fitting, and make the model more generalizable, we utilize compression at a rate of 0.5.

d) Fully Connected Layers: The model's final section contains two fully connected layers: the first flattens the feature maps using global average pooling into a long 1D array of 360 nodes, which is then fed to the second fully connected layer as a two classifier, which contains two neurons, one for has-IDC and the other for no-IDC.

IV. RESULTS AND DISCUSSION

The accuracy, loss, balanced accuracy, and several other parameters such as Precision, Recall, F1 score, and sensitivity/specificity were employed to evaluate the tumor binary classification performance. Gradient weighted class activation maps (Grad-CAM) are also used to visualize the model and produce a heat map for a better understanding of the region of interest. For the best output of the neural network, fine-tuning was done by adjusting the kernel dimensions and the number of dense modules. The kernel sizes were (1×1), (3×3) and (7×7). respectively. Since there was no need to learn duplicate feature maps, the number of dense blocks ranged from one to three, enabling the collective knowledge to be reused.

International Journal of Engineering Research & Technology (IJERT)
ISSN: 2278-0181
Vol. 10 Issue 11, November-2021

A. *Experimental Setup*

We developed our framework utilizing Python as the programming language and a variety of open-source software packages and libraries, including TensorFlow 1.12.0 [48], [40] and Keras [41]. An NVIDIA® GTX 1060 6GB/PCIe/SSE2 GPU was used to train the CNN models. Keras. callbacks were used to monitor the experiments. The ModelCheckpoint class is used to save model checkpoints. This class has two objects defined since it's a two classification problem. The first goal is to save the model called the last Weights model after each epoch, and the second goal is to save the best weights. During training, we fed the network 50x50 patches of RGB images that were resized to 100x100 after our hybrid preprocessing phase normalized between 0 and 1 and trained it for a two classification tumor problem with a batch size of 32 and cross-entropy loss during training. With a learning rate of 10exp-2, we used Adam optimization and gradually decreased it as the training progressed. The model was trained on 331569 images, with data imbalance augmentation, validation 9035 images, and testing 904 images.

B. *Confusion Matrix and Performance scores*

Figure 5 depicts the confusion matrix. It indicates how well the proposed model performed on the test set. The confusion matrix is based on a model with three dense blocks composed of convolutional layers with kernel dimensions of (7×7). The following Table.2 shows the performance metrics obtained from the aforementioned confusion matrix.

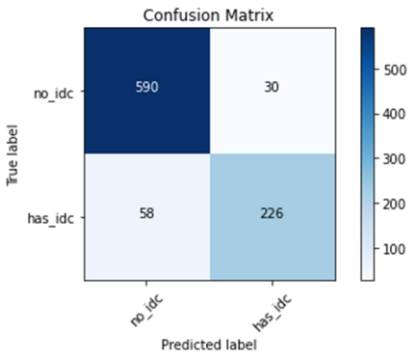

Fig. 5 Confusion Matrix of the proposed network

TABLE II. THE CLASSIFICATION RESULTS FOR POSITIVE AND NEGATIVE INVASIVE DUCTAL CARCINOMA

Class	Precision	Recall	F1-SCORE	Support
No_idc (-)	0.91	0.95	0.93	620
Has_idc (+)	0.88	0.80	0.83	284
Accuracy			0.90	904
Macro avg	0.89	0.87	0.88	904
Weighted avg	0.90	0.90	0.90	904

TABLE III. SHOWS SENSITIVITY AND SPECIFICITY OF IDC DETECTION

Accuracy	**90%**
Sensitivity	**80%**
Specificity	**95%**

According to the results in Table.3, our automated two-classification IDC breast cancer detector obtains 90% precision on our sample dataset. It also achieves 80% sensitivity and 95% specificity, meaning that patients who have IDC (i.e., true positive) could be accurately identified as "IDC positive" 80% of the time, while patients that do not have IDC (i.e., true negative) could be accurately identified as "IDC negative" only 95% of the time using our model.

TABLE IV. THE F-SCORE AND BALANCE ACCURACY OF OUR METHOD VS STING DEEP LEARNING APPROACHES

Study	Year	Input Size	Method	F-Score (%)	BAC (%)
Cruz-Roa et al. [6]	2014	50 × 50	3-layer CNN	71.80	84.23
Janowczyk et al. [42]	2016	32 × 32	AlexNet	76.48	84.68
Bejnordi et al. [43]	2017	768×768	Stacked CNN for classification		81.3
Reza et al. [23]	2018	50 × 50	SMOTE+CNN	84.78	85.48
Romano et al. [7]	2019	50x50	Enhanced Deep Learning Approach	85.28	85.41
Seemendra et al. [44]	2020		Transfer learning with deep learning architectures	87.46	86.97
Our Method	-	100x100	Densenet + A hybrid pre-processing	88.0	87.2

In comparison to the currently published methods on IDC classification approaches, we can see that quantitatively presenting the F-score and balanced accuracy for our approach in Table.4 provides a better F-score and slightly higher balanced accuracy. The proposed methodology and network's optimal performance are also validated by the other performance metrics

C. *Grad-CAM Visualization*

To validate the model's classification ability, the Gradient weighted class activation maps (Grad-CAM) for each convolutional layer were monitored. The class activation maps in the dataset's histopathology images aid in visualizing the affected regions. The Grad-CAM algorithm generates a heat map that represents the region of interest while retaining spatial information that would otherwise be lost in the dense or FC layers of the model. In Fig. 6, the Grad-CAMs of the dense

International Journal of Engineering Research & Technology (IJERT)
ISSN: 2278-0181
Vol. 10 Issue 11, November-2021

network's final convolutional layer is seen alongside the original processed images for a few images from the test collection. The model learning performance curves are shown in fig.7

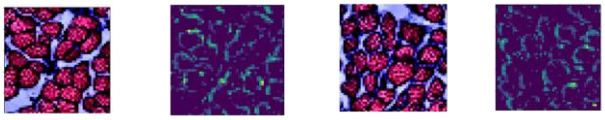

Fig. 6 Shows Grad-CAM visualization of the images (Left: Original processed images; Right: Grad-CAM heat map of the region of interest of the images)

Fig. 7 Shows the learning curves of our model. In blue training and red validation accuracy curves on the left. The right part shows the training loss in blue and validation loss in red color.

V. CONCLUSION AND FUTURE SCOPE

In this paper, an enhanced approach is utilized for predicting Invasive Ductal Carcinoma (IDC) from breast cancer histopathology images using Dense Convolutional Neural Networks. The incorporated hybrid preprocessing technique based on color normalization, denoising, adaptive gamma correction, followed by contrast limited adaptive histogram equalization (CLAHE) makes the model more optimum in terms of its classification ability. The comparative study with the existing statistical models illustrated in Table.4, shows that the proposed model has better performance than existing models for IDC classification in breast cancer histopathology images. It also provides the merit to the different channels in the images that can be fed to any deep learning model. The dense network incorporated in the proposed methodology ensures stronger feature propagation, feature reuse, reduced parameter count, alleviates the problem of vanishing gradient and accuracy degradation with the increase in depth of the model. Such models can be applied in research and diagnosis of various diseases like COVID-19 pandemic.

Deep learning for image classification is an iterative process. During model monitoring when we implemented image augmentation, we observed that histopathology images of breast cancer are inherently symmetrical under rotation. However, this rotational symmetry is not widely utilized as prior information in the Convolutional Neural Networks (CNNs), resulting in hungry data and independent feature learning at each orientation. As future work, it is intended to extend the model's classification ability approach to utilizing rotation-equivalent CNNs, and eliminate the need to learn this series of transformations from data, hence allowing more discriminative features to be studied. It is also intended to make the proposed model a state-of-the art algorithm for the classification of various histopathology images.

REFERENCES

[1] C. P. Stewart, B. W., Wild, "World Cancer Report 2014 - WHO - OMS -," *World Heal. Organ. Press*, 2014.

[2] Breastcancer.org, "Invasive Ductal Carcinoma: Diagnosis, Treatment, and More.," *breastcancer.org*.

[3] American Cancer Society, "Invasive Breast Cancer (IDC/ILC): Types of Invasive Breast Carcinoma," *cancer.org*.

[4] M. Veta, J. P. W. Pluim, P. J. Van Diest, and M. A. Viergever, "Breast cancer histopathology image analysis: A review," *IEEE Trans. Biomed. Eng.*, 2014, doi: 10.1109/TBME.2014.2303852.

[5] M. T. McCann, J. A. Ozolek, C. A. Castro, B. Parvin, and J. Kovačević, "Automated Histology Analysis: Opportunities for signal processing," *IEEE Signal Processing Magazine*. 2015.

[6] A. Cruz-Roa *et al.*, "Automatic detection of invasive ductal carcinoma in whole slide images with convolutional neural networks," 2014.

[7] A. M. Romano and A. A. Hernandez, "Enhanced Deep Learning Approach for Predicting Invasive Ductal Carcinoma from Histopathology Images," 2019.

[8] R. Sanyal, D. Kar, and R. Sarkar, "Carcinoma type classification from high-resolution breast microscopy images using a hybrid ensemble of deep convolutional features and gradient boosting trees classifiers," *IEEE/ACM Trans. Comput. Biol. Bioinforma.*, p. 1, 2021.

[9] R. Bhargava and A. Madabhushi, "Emerging themes in image informatics and molecular analysis for digital pathology," *Annu. Rev. Biomed. Eng.*, vol. 18, pp. 387–412, 2016.

[10] F. A. Zeiser, C. A. da Costa, A. V. Roehe, R. da R. Righi, and N. M. C. Marques, "Breast cancer intelligent analysis of histopathological data: A systematic review," *Appl. Soft Comput.*, vol. 113, p. 107886, Dec. 2021.

[11] R. Krithiga and P. Geetha, "Breast Cancer Detection, Segmentation and Classification on Histopathology Images Analysis: A Systematic Review," *Arch. Comput. Methods Eng.*, vol. 28, no. 4, pp. 2607–2619, 2021.

[12] I. O. Sigirci, A. Albayrak, and G. Bilgin, "Detection of mitotic cells in breast cancer histopathological images using deep versus handcrafted features," *Multimed. Tools Appl.*, 2021.

[13] S. S. Chaturvedi, J. V Tembhurne, and T. Diwan, "A multi-class skin Cancer classification using deep convolutional neural networks," *Multimed. Tools Appl.*, vol. 79, no. 39, pp. 28477–28498, 2020.

[14] W. Wang *et al.*, "Medical image classification using deep learning," in *Deep Learning in Healthcare*, Springer, 2020, pp. 33–51.

[15] J. Noorbakhsh *et al.*, "Deep learning-based cross-classifications reveal conserved spatial behaviors within tumor histological images," *Nat. Commun.*, vol. 11, no. 1, p. 6367, 2020.

[16] Y. LeCun, L. Bottou, Y. Bengio, and P. Haffner, "Gradient-based learning applied to document recognition," *Proc. IEEE*, 1998.

International Journal of Engineering Research & Technology (IJERT)
ISSN: 2278-0181
Vol. 10 Issue 11, November-2021

[17] T. Hayakawa, V. B. S. Prasath, H. Kawanaka, B. J. Aronow, and S. Tsuruoka, "Computational Nuclei Segmentation Methods in Digital Pathology: A Survey," *Arch. Comput. Methods Eng.*, vol. 28, no. 1, pp. 1–13, 2021.

[18] G. Huang, Z. Liu, L. Van Der Maaten, and K. Q. Weinberger, "Densely connected convolutional networks," 2017.

[19] K. Lan, D. tong Wang, S. Fong, L. sheng Liu, K. K. L. Wong, and N. Dey, "A Survey of Data Mining and Deep Learning in Bioinformatics," *Journal of Medical Systems*. 2018.

[20] S. Kalra *et al.*, "Pan-cancer diagnostic consensus through searching archival histopathology images using artificial intelligence," *npj Digit. Med.*, vol. 3, no. 1, p. 31, 2020, doi:.

[21] S. Doyle, S. Agner, A. Madabhushi, M. Feldman, and J. Tomaszewski, "Automated grading of breast cancer histopathology using spectral clustering with textural and architectural image features," 2008.

[22] S. Naik, S. Doyle, S. Agner, A. Madabhushi, M. Feldman, and J. Tomaszewski, "Automated gland and nuclei segmentation for grading of prostate and breast cancer histopathology," 2008.

[23] M. S. Reza and J. Ma, "Imbalanced histopathological breast cancer image classification with convolutional neural network," 2019.

[24] B. Ehteshami Bejnordi *et al.*, "Automated Detection of DCIS in Whole-Slide H&E Stained Breast Histopathology Images," *IEEE Trans. Med. Imaging*, 2016.

[25] B. E. Bejnordi *et al.*, "Context-aware stacked convolutional neural networks for classification of breast carcinomas in whole-slide histopathology images," *J. Med. Imaging*, 2017.

[26] S. Roy, A. kumar Jain, S. Lal, and J. Kini, "A study about color normalization methods for histopathology images," *Micron*. 2018.

[27] D. Onder, S. Zengin, and S. Sarioglu, "A review on color normalization and color deconvolution methods in histopathology," *Applied Immunohistochemistry and Molecular Morphology*. 2014.

[28] R. Silpasai, H. Singh, A. Kumar, and L. K. Balyan, "Homomorphically Rectified Tile-wise Equalized Adaptive Gamma Correction for Histopathological Color Image Enhancement," 2018.

[29] K. G. Dhal, S. Ray, S. Das, A. Biswas, and S. Ghosh, "Hue-Preserving and Gamut Problem-Free Histopathology Image Enhancement," *Iran. J. Sci. Technol. - Trans. Electr. Eng.*, 2019.

[30] M. Kohl, C. Walz, F. Ludwig, S. Braunewell, and M. Baust, "Assessment of Breast Cancer Histology Using Densely Connected Convolutional Networks," 2018.

[31] P. Mooney, "Breast Histopathology Images," *kaggle.com*. https://www.kaggle.com/paultimothymooney/breast-histopathology-images (accessed Sep. 26, 2020).

[32] M. Macenko *et al.*, "A method for normalizing histology slides for quantitative analysis," 2009.

[33] T. G. Devi and N. Patil, "Analysis & Evaluation of Image filtering Noise reduction technique for Microscopic Images," in *2020 International Conference on Innovative Trends in Information Technology (ICITIIT)*, Feb. 2020, pp. 1–6.

[34] Y. Lee, S. Zhang, M. Li, and X. He, "Blind Inverse Gamma Correction with Maximized Differential Entropy," *arXiv Prepr. arXiv2007.02246*, 2020.

[35] S. Rahman, M. M. Rahman, M. Abdullah-Al-Wadud, G. D. Al-Quaderi, and M. Shoyaib, "An adaptive gamma correction for image enhancement," *Eurasip J. Image Video Process.*, 2016.

[36] D. A. Clevert, T. Unterthiner, and S. Hochreiter, "Fast and accurate deep network learning by exponential linear units (ELUs)," 2016.

[37] M. Kabkab, E. Hand, and R. Chellappa, "On the size of Convolutional Neural Networks and generalization performance," in *2016 23rd International Conference on Pattern Recognition (ICPR)*, Dec. 2016, pp. 3572–3577.

[38] T.-Y. Hsiao, Y.-C. Chang, H.-H. Chou, and C.-T. Chiu, "Filter-based deep-compression with global average pooling for convolutional networks," *J. Syst. Archit.*, vol. 95, pp. 9–18, 2019.

[39] S. Suita *et al.*, "Efficient convolution pooling on the GPU," *J. Parallel Distrib. Comput.*, vol. 138, pp. 222–229, 2020.

[40] M. Abadi *et al.*, "TensorFlow: A system for large-scale machine learning," 2016.

[41] K. (n. d. . Team, "Keras," *keras.io*. https://keras.io/ (accessed Sep. 26, 2020).

[42] A. Janowczyk and A. Madabhushi, "Deep learning for digital pathology image analysis: A comprehensive tutorial with selected use cases," *J. Pathol. Inform.*, 2016.

[43] B. Ehteshami Bejnordi *et al.*, "Deep learning-based assessment of tumor-associated stroma for diagnosing breast cancer in histopathology images," 2017.

[44] A. Seemendra, R. Singh, and S. Singh, "Breast Cancer Classification Using Transfer Learning," in *Evolving Technologies for Computing, Communication and Smart World*, Springer, pp. 425–436.